^{1}H NMR Spectroscopy and the Electronic Structure of the High Potential Iron-Sulfur Protein from *Chromatium vinosum*

Ivano Bertini,*,† Fabrizio Briganti,† Claudio Luchinat,‡ Andrea Scozzafava,† and Marco Sola§

Contribution from the Department of Chemistry, University of Florence, Via Gino Capponi 7, 50121 Florence, Italy, Institute of Agricultural Chemistry, University of Bologna, Viale Berti Pichat 10, 40127 Bologna, Italy, and Department of Chemistry, University of Modena, Via Campi 183, 41100 Modena, Italy. *Received May 10, 1990*

Abstract: ^{1}H NMR and NOE measurements have been performed on reduced HiPIP from *Chromatium vinosum*. 1D and 2D saturation transfer experiments have allowed a full correlation between the isotropically shifted signals of the reduced and oxidized species. The pairwise assignment of the cysteine geminal β-CH_2 protons is performed. This allows the relative evaluation of the expectation value $\langle S_{iz} \rangle$ for each iron ion i as well as its temperature dependence. A theoretical approach has been able to account for upfield shifts of β-CH_2 cysteine protons in the oxidized species. The ^{1}H NMR data turn out to be a valuable benchmark for testing theoretical models for Fe_4S_4 clusters. The present model supports the existence of a mixed-valence pair with $S = {}^9/_2$ ground state in the oxidized protein and is consistent with the presence of analogous mixed-valence pairs also in the reduced protein. The NMR data on the oxidized protein also show that, even at room temperature, electron delocalization mainly occurs within one particular Fe(II)-Fe(III) pair.

Introduction

The understanding of the electronic structure of Fe_4S_4 clusters in proteins is a challenging task nowadays. The experimental data available come from Mössbauer, ^{1}H NMR, and magnetic spectroscopies. Mössbauer data have been of fundamental importance; however the data are available only at around liquid helium temperature, thus providing information only on the ground state.[1-7] The magnetic susceptibility data are still at a pioneeristic level owing to the difficulties of measuring paramagnetic contributions in the presence of the large diamagnetic contribution from the protein.[8-13] MCD spectral data may also be helpful in understanding the magnetic properties of the ground state and low-lying excited states.[14] However, no conclusive information is as yet available on Fe_4S_4 systems.[15,16] The ^{1}H NMR spectra in solution provide hyperfine shifts which are proportional to the isotropic hyperfine coupling between the unpaired electrons present on each metal ion and the resonating protons and to the experimental value of $\langle S_{iz} \rangle$ for each ion i sensed by the proton.[17] The latter value depends on the pattern of the electronic levels originated by the magnetic coupling within the cluster and on their population as it changes with temperature according to Boltzmann law.

Hyperfine shifted signals of various Fe_4S_4 proteins have been reported but up to now not fully understood.[18-25] Through steady-state ^{1}H NOE measurements the Cys β-CH_2 geminal protons can be pairwise assigned.[26-28] We are going to show here that calculations based on Heisenberg AF exchange allow us to predict the hyperfine shifts of the β-CH_2 protons and to obtain a deeper insight into the electronic structure of these clusters. Indeed, the approach was first suggested by Palmer et al. for the interpretation of reduced Fe_2S_2 proteins containing Fe(II)-Fe(III) antiferromagnetically coupled.[29] On this basis some of us had looked for and found the four missing hyperfine shifted proton signals of the protein,[26,30] thus giving a full account of the relationships between NMR parameters and the electronic structure of the clusters.[31] We then successfully accounted for the electronic properties of Co_4S_4 clusters in cobalt(II)-substituted thioneins through ^{1}H NMR spectra.[32,33]

* Address correspondence to this author at Department of Chemistry, University of Florence, Via G. Capponi 7, 50121 Florence, Italy.
† University of Florence.
‡ University of Bologna.
§ University of Modena.

⊥ Abbreviations used throughout this paper: AF, antiferromagnetic; *Ch.v.*, *Chromatium vinosum*; EXSY, 2-D NMR exchange spectroscopy; Fd, ferredoxin; HiPIP, high potential iron-sulfur protein; MoDEFT, modified driven equilibrium Fourier transform; NMR, nuclear magnetic resonance; NOE, nuclear Overhauser effect; P_i, phosphate; ppm, parts per million; WEFT, water eliminated Fourier transform.

(1) Munck, E.; Huynh, B. H. In *ESR and NMR of Paramagnetic Species in Biological and Related Systems*; Bertini, I., Drago, R. S., Eds.; D. Reidel Publishing Co.: 1979; Chapter 12.
(2) Middleton, P.; Dickson, D. P. E.; Johnson, C. E.; Rush, J. D. *Eur. J. Biochem.* **1980**, *104*, 289-296.
(3) Moss, T. H.; Bearden, A. J.; Bartsch, R. G.; Cusanovich, M. A. *Biochemistry* **1968**, *7*, 1591-1596.
(4) Dickson, D. P. E.; Johnson, C. E.; Cammack, R.; Evans, M. C. W.; Hall, D. O.; Kao, K. K. *Biochem. J.* **1974**, *139*, 105-108.
(5) Thompson, C. L.; Johnson, C. E.; Dickson, D. P. E.; Cammack, R.; Hall, D. O.; Weser, U.; Kao, K. K. *Biochem. J.* **1974**, *139*, 97-103.
(6) Middleton, P.; Dickson, D. P. E.; Johnson, C. E.; Rush, J. D. *Eur. J. Biochem.* **1978**, *88*, 135-141.
(7) Christner, J. A.; Janick, P. A.; Siegel, L. M.; Munck, E. *J. Biol. Chem.* **1983**, *258*, 11157-11164.
(8) Hall, D. O. In *Bioinorganic Chemistry*; Raymond, K. N., Ed.; Advances in Chemistry Series 162, American Chemical Society: Washington, DC, 1977; Vol. 2, Chapter 13.
(9) Phillips, W. D.; McDonald, C. C.; Stombaugh, N. A.; Orme-Johnson, W. H. *Proc. Natl. Acad. Sci. U.S.A.* **1974**, *71*, 140-143.
(10) Orme-Johnson, W. H. In *Inorganic Biochemistry*; Eichhorn, G. L., Ed., Elsevier: 1973; Vol. 2, Chapter 22.
(11) Antanaitis, B. C.; Moss, T. H. *Biochim. Biophys. Acta* **1975**, *405*, 262-279.
(12) Poe, M.; Phillips, W. D.; McDonald, C. C.; Lovenberg, W. *Proc. Natl. Acad. Sci. U.S.A.* **1970**, *65*, 797.
(13) Poe, M.; Phillips, W. D.; McDonald, C. C.; Orme-Johnson, W. H. *Biochem. Biophys. Res. Commun.* **1971**, *42*, 705-713.
(14) Thomson, A. J.; Robinson, A. E.; Johnson, M. K.; Moura, J. J. G.; Moura, I.; Xavier, A. V.; LeGall, J. *Biochem. Biophys. Acta* **1981**, *670*, 93-100.
(15) Stephens, P. J.; Thomson, A. J.; Dunn, J. B. R.; Keiderling, T. A.; Rawlings, J.; Rao, K. K.; Hall, D. O. *Biochemistry* **1978**, *17*, 4770-4778.
(16) Ulmer, D. D.; Holmquist, B.; Vallee, B. R. *Biochem. Biophys. Res. Commun.* **1973**, *51*, 1054.
(17) Bertini, I.; Luchinat, C. *NMR of Paramagnetic Molecules in Biological Systems*; Benjamin/Cummings: Menlo Park, CA, 1986.
(18) Phillips, W. D.; In *NMR of Paramagnetic Molecules, Principles and Applications*; La Mar, G. N., Horrocks, W. DeW. Jr., Holm, R. H., Eds.; Academic Press: New York, 1973; Chapter 11.
(19) Packer, E. L.; Sweeny, W. V.; Rabinowitz, J. C.; Sternlicht, H.; Shaw, E. N. *J. Biol. Chem.* **1977**, *252*, 2245.
(20) Phillips, W. D.; Poe, M. In *Iron-Sulfur Proteins*; Lovenberg, W., Ed.; Academic Press: New York, 1977; Vol. 3, Chapter 7.
(21) Gaillard, J.; Moulis, J.-M.; Meyer, J. *Inorg. Chem.* **1987**, *26*, 320.
(22) Nettesheim, D. G.; Meyer, J. L.; Feinberg, B. A.; Otvos, J. D. *J. Biol. Chem.* **1983**, *258*, 8235.
(23) Krishnamoorthi, R.; Markley, J. L.; Cusanovich, M. A.; Prysiecki, C. T.; Meyer, T. E. *Biochemistry* **1986**, *25*, 60.
(24) Krishnamoorthi, R.; Cusanovich, M. A.; Meyer, T. E.; Prysiecki, C. T. *Eur. J. Biochem.* **1989**, *181*, 81.
(25) Sola, M.; Cowan, J. A.; Gray, H. B. *Biochemistry* **1989**, *28*, 5261-5268.

0002-7863/91/1513-1237$02.50/0

The presence of mixed valence pairs observed in Fe_3S_4 and Fe_4S_4 clusters through Mössbauer experiments has been recently accounted for by adding a double exchange term[34-36] to the Heisenberg AF Hamiltonian. This term contributes to the stabilization of the $S = {}^9/_2$ ground state for the mixed valence pair.[34-36] While the present data are in agreement with the presence of such a ground state, they cannot be used to establish the relative importance of "spin frustration"[34] effects—already present in the pure Heisenberg AF model—versus double exchange in yielding an $S = {}^9/_2$ ground state for the mixed-valence pair.

The published ^{1}H NMR spectra of Fe_4S_4 clusters in the various oxidation states can now be interpreted and the essential features accounted for.[27,31] We have measured the ^{1}H NMR spectra and the ^{1}H NOE of reduced Fe_4S_4 from *Chromatium vinosum*—which formally contains two Fe(II) and two Fe(III) ions—to assign all the β-CH_2 cysteinyl geminal protons, and through saturation transfer experiments we have connected the isotropically shifted signals of reduced and one-electron oxidized protein. Together with the previously reported ^{1}H NOE data of the latter,[28] the present data allow a full assignment of the cysteine β-CH_2 protons of both species.

Experimental Section

All chemicals used throughout were of the best quality available. *Chromatium vinosum* HiPIP was purified as previously reported.[37] Experiments in D_2O 99.95%, 30 mM NaP_i were performed by solvent exchange utilizing an ultrafiltration Amicon cell equipped with a YM5 membrane; at least five changes of deuterated buffer were performed to assure satisfactory solvent exchange. The protein samples (1–4 mM) were reduced or oxidized by addition of small amounts of 0.1 M sodium dithionite or potassium hexacyanoferrate(III), respectively, in 30 mM NaP_i, D_2O 99.9%; the extent of reduction/oxidation was monitored by measuring the area of the NMR peaks corresponding to the different redox species. The pH values are reported as uncorrected pH meter readings.

High-resolution Fourier transform ^{1}H NMR measurements were carried out on a Bruker AC-P 300 spectrometer running at 300 MHz. Typically 1000–5000 transients were acquired utilizing the MoDEFT (90-τ-180-τ-90-AQ) or super-WEFT (180-τ-90-AQ) pulse sequences.[38,39]

^{1}H NOE and saturation transfer measurements were performed by collecting 2–16 K data points over 15–75 KHz bandwidths. The water signal was suppressed by using the super-WEFT pulse sequence with recycle times of 90–140 ms and delay times τ of 70–120 ms. The resonances under investigation were saturated by utilizing a selective decoupling pulse of 0.01–0.02 W kept on for 9/10 of the delay time τ. Difference spectra were collected directly by applying the decoupler frequency alternatively according to the scheme

$$\omega_2\text{—}(\omega_2 + \delta)\text{—}\omega_2\text{—}(\omega_2 - \delta)$$

where ω_2 is the frequency of the irradiated signal and δ is a small off-resonance offset, typically of the order of twice the irradiated signal line width; the receiver phase was alternated in such a way that the scans with the decoupler frequency on-resonance were added, and those with the decoupler frequency off-resonance subtracted. This sequence scheme allows the obtaining of good difference spectra minimizing hardware instabilities. Each experiment, run in block-averaging mode, consisted usually of 30–50 blocks of 4096 scans each. Exponential multiplication of the free induction decay improved the signal-to-noise ratio introducing 5–15 Hz additional line broadening.

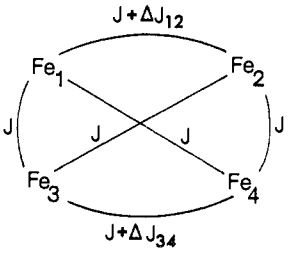

Figure 1. Heisenberg–AF exchange coupling scheme for Fe_4S_4 clusters.

T_1 measurements were performed by utilizing either the MoDEFT or inversion recovery sequences.[38,40] 2D NMR EXSY spectra[41,42] were acquired with the pulse sequence D1-180-τ-90-t1-90-τ_m-90-AQ, where the super-WEFT pulse sequence is followed by the standard NOESY sequence. EXSY experiments were recorded with 1K data points in t2 and 256 t1 values with 4000 scans per FID. In the experiment reported D1 = 73 ms, τ = 80 ms, τ_m = 7.5 ms, and AQ = 7 ms. Prior to Fourier transformation the 2D data matrix was multiplied by a cosine bell function in both t1 and t2.

Nuclear Overhauser Effect and Saturation Transfer

The nuclear Overhauser effect is defined as the fractional intensity change of a NMR resonance i upon saturation of another resonance j in the same molecular species. The steady-state NOE η_{ij} is given by[43,44]

$$\eta_{ij} = \sigma_{ij}/\rho_i \tag{1}$$

where ρ_i is the intrinsic relaxation spin–lattice rate for the nucleus i and σ_{ij} is the cross relaxation rate between i and j given by

$$\sigma_{ij} = -\frac{\hbar^2\gamma^4}{10r_{ij}^6} f(\tau_c) \tag{2}$$

where, if local motions are not present, τ_c is the protein tumbling time, and r_{ij} is the internuclear distance. In the present case $f(\tau_c) = \tau_c$.

NOEs in paramagnetic systems are relatively difficult to observe because the large intrinsic longitudinal relaxation rates ρ_i make η_{ij} small.[43-47] However, the paramagnetism quenches spin diffusion allowing the selective detection of primary NOEs in large proteins.[45-47] In the present system the ρ_i values of the isotropically shifted resonances are between 500 and 40 s^{-1}; using a τ_r value of 3.3×10^{-9} s, as calculated from the Stokes–Einstein equation for isotropic rotational motion of a 10000 MW protein, interproton distances of 1.7–1.9 Å are estimated from the experimental NOE values and are consistent with β-CH_2 geminal protons.

Furthermore, signals belonging to the same nuclear species which interconverts between two different chemical environments on a time scale comparable with the intrinsic relaxation times may lead through magnetization transfer experiments to establish

(26) Dugad, L. B.; La Mar, G. N.; Banci, L.; Bertini, I. *Biochemistry* **1990**, *29*, 2263–2271.
(27) Bertini, I.; Briganti, F.; Luchinat, C.; Scozzafava, A. *Inorg. Chem.* **1990**, *29*, 1874.
(28) Cowan, J. A.; Sola, M. *Biochemistry* **1990**, *29*, 5633.
(29) Dunham, W. R.; Palmer, G.; Sands, R. H.; Bearden, A. J. *Biochim. Biophys. Acta* **1971**, *253*, 373–384.
(30) Bertini, I.; Lanini, G.; Luchinat, C. *Inorg. Chem.* **1984**, *23*, 2729.
(31) Banci, L.; Bertini, I.; Luchinat, C. *Structure and Bonding* **1990**, *72*, 113–135.
(32) Bertini, I.; Luchinat, C.; Messori, L.; Vasak, M. *J. Am. Chem. Soc.* **1989**, *111*, 7296–7300.
(33) Bertini, I.; Luchinat, C.; Messori, L.; Vasak, M. *J. Am. Chem. Soc.* **1989**, *111*, 7300–7303.
(34) Münck, E.; Papaefthymiou, V.; Surerus, K. K.; Girerd, J. J. In *Metals in Proteins*; Que, L., Ed.; ACS Symposium Series; American Chemical Society: Washington, DC, 1988; and references therein.
(35) Papaefthymiou, V.; Girerd, J.-J.; Moura, I.; Moura, J. J. G.; Munck, E. *J. Am. Chem. Soc.* **1987**, *109*, 4703–4710.
(36) Noodleman, L. *Inorg. Chem.* **1988**, *27*, 3677–79.
(37) Bartsch, R. G. *Methods Enzymol.* **1978**, *53*, 329.
(38) Hochmann, J.; Kellerhals, H. *J. Magn. Reson.* **1980**, *38*, 23.
(39) Inubushi, T.; Becker, E. D. *J. Magn. Reson.* **1983**, *51*, 128.
(40) Vold, R. L.; Waugh, J. S.; Klein, M. P.; Phelps, D. E. *J. Chem. Phys.* **1968**, *48*, 3831.
(41) Bodenhausen, G.; Ernst, R. R. *J. Am. Chem. Soc.* **1982**, *104*, 1304.
(42) Ernst, R. R.; Bodenhausen, G.; Wokaun, A. *Principles of Nuclear Magnetic Resonance in One and Two Dimensions*; Clarendon Press: Oxford, 1987; p 490. Jenkins, B. J.; Lauffer, R. B. *Inorg. Chem.* **1988**, *27*, 4730–4738.
(43) Noggle, J. H.; Shirmer, R. E. *The Nuclear Overhauser Effect*; Academic: New York, 1971.
(44) Neuhaus, D.; Williamson, M. *The Nuclear Overhauser Effect in Structural and Conformational Analysis*; VCH Publ.: New York, 1989.
(45) Dugad, L. B.; La Mar, G. N.; Unger, S. W. *J. Am. Chem. Soc.* **1990**, *112*, 1386–1392.
(46) Thanabal, V.; de Ropp, J. S.; La Mar, G. N. *J. Am. Chem. Soc.* **1987**, *109*, 265–272.
(47) Unger, S. W.; Lecompte, J. T.; La Mar, G. N. *J. Magn. Reson.* **1985**, *64*, 521–526.

connectivities between resonances and to extend known assignments in one chemical environment to the other environment in equilibrium with the former. In the case of two species in equilibrium A ⇌ B, by presaturating the B resonance a decrease in intensity of the A resonance is obtained. The relation connecting the intensity of the signal, which is proportional to M_z^A; and the exchange time τ is[17,48,49]

$$\tau = T_1^A \frac{M_z^A/M_0^A}{1 - M_z^A/M_0^A} \quad (3)$$

where M_z^A and M_0^A are the magnetizations observed with and without irradiation of signal B, respectively, and T_1^A is the intrinsic spin-lattice relaxation time for the nucleus in the A environment in the absence of exchange. In 2D EXSY experiments mixing times τ_m of the order of $T_1^{A,B}$ are needed, and the cross peak intensity depends on the exchange time τ[41,42]

$$M_z^A = M_0^A\,[1 - e^{(-\tau/\tau_m)}]e^{(-\tau/T_1)}/2 \quad (4)$$

Theoretical Considerations

The scheme of the Fe_4S_4 cluster is shown in Figure 1. We have first considered the following Heisenberg-Dirac-Van Vleck spin Hamiltonian to parametrize the exchange interaction between the iron center

$$\mathcal{H} = J(\mathbf{S}_1\cdot\mathbf{S}_2 + \mathbf{S}_1\cdot\mathbf{S}_3 + \mathbf{S}_1\cdot\mathbf{S}_4 + \mathbf{S}_2\cdot\mathbf{S}_3 + \mathbf{S}_2\cdot\mathbf{S}_4 + \mathbf{S}_3\cdot\mathbf{S}_4) + \Delta J_{12}(\mathbf{S}_1\cdot\mathbf{S}_2) + \Delta J_{34}(\mathbf{S}_3\cdot\mathbf{S}_4) \quad (5)$$

where S_1, S_2, S_3, and S_4 are the spin numbers of the different iron centers, J is the iron-iron isotropic exchange coupling constant, and ΔJ_{12} and ΔJ_{34} are the deviations from J of the exchange coupling constants between the iron centers in the 1-2 and 3-4 pairs (refer to the labeling of Figure 1). In this way, up to three different J values can be considered, and analytical solutions can be obtained. The corresponding expression for the energies of the levels are

$$E(S_{12}S_{34}S) = (J/2)[S(S+1)] + (\Delta J_{12}/2)[S_{12}(S_{12}+1)] + (\Delta J_{34}/2)[S_{34}(S_{34}+1)] \quad (6)$$

where $S = S_1 + S_2 + S_3 + S_4$, $S_{12} = S_1 + S_2$, and $S_{34} = S_3 + S_4$.

A formal attribution of the oxidation states to the individual iron centers shows that the cluster is formed by iron(II) and iron(III) centers. This picture is not consistent, anyway, with the Mössbauer spectra of such clusters, and a better picture should include electron delocalization of the magnetic electrons over the spin centers.[34-36] The effect of the delocalization of the magnetic electrons provides a coupling mechanism, often referred to as double exchange, which in principle is different from the isotropic Heisenberg-Dirac-Van Vleck spin coupling. In dinuclear systems this effect was already studied by Zener[50] and Anderson and Hasegawa[51] and more recently by Karpenko,[52] Girerd,[53] Belinskii,[54] and Noodleman.[55] Girerd has recently established the theoretical basis for the introduction of the double exchange operator in the spin Hamiltonian formalism.[56] The delocalization was found to produce a resonance splitting of the total spin multiplets arising from the isotropic exchange stabilizing the highest spin state for mixed-valence pairs, thus providing a ferromagnetic contribution to the exchange interaction. For trinuclear mixed-valence systems Belinskii found a similar splitting,[57] but the actual spin level ordering was found to depend more critically on the p/J ratio, where p is the transfer integral and J is the exchange parameter. In low symmetry systems the extent of double exchange can hardly be quantitated from magnetic measurements alone, and a number of mixed-valence clusters have been analyzed by using the simpler Heisenberg-Dirac-Van Vleck spin Hamiltonian.[58-60] The mixed-valence character of some iron clusters was recognized through magnetic Mössbauer measurements which show intermediate oxidation states for the iron ions.[34,35]

One (for $Fe_4S_4^{3+}$ clusters) or two (for $Fe_4S_4^{2+}$ clusters) delocalization terms B can be semiempirically taken into consideration by adding extra terms to the energy expression 6[36,61]

$$E(S_{12}S_{34}S) = (J/2)[S(S+1)] \pm B_{12}(S_{12}+\tfrac{1}{2}) \pm B_{34}(S_{34}+\tfrac{1}{2}) + (\Delta J_{12}/2)[S_{12}(S_{12}+1)] + (\Delta J_{34}/2)[S_{34}(S_{34}+1)] \quad (7)$$

We are then going to calculate the hyperfine shifts as given by

$$A\langle \mathbf{S}_{iz}\rangle / \langle \mathbf{S}_z\rangle \quad (8)$$

where A, the hyperfine coupling constant between each of the β-CH_2 protons and the paramagnetic center is taken equal and positive for iron(II), iron(III), or mixed-valence iron, and the $\langle \mathbf{S}_{iz}\rangle$ values for each energy level depend on the Hamiltonian (5)

$$\langle \mathbf{S}_{iz}\rangle / \langle \mathbf{S}_z\rangle = \alpha_i\gamma_i/\Delta_i \quad (9)$$

where

$$\alpha_i = \{\beta_1[S_{ij}(S_{ij}+1) + S_i(S_i+1) - S_j(S_j+1)] + \beta_2[S_{ij}(S_{ij}+1) - S_i(S_i+1) + S_j(S_j+1)]\}/2$$

$$\gamma_i = [S(S+1) + S_{ij}(S_{ij}+1) - S_{kl}(S_{kl}+1)]/2$$

$$\Delta_i = S_{ij}(S_{ij}+1)S(S+1)$$

and i and j correspond to the iron sites of one pair (1-2 or 3-4), whereas k and l to the iron sites of the other pair. Furthermore, $\beta_1 = \beta_2 = {}^1/_2$ in the presence of double exchange or $\beta_1 = 1$ and $\beta_2 = 0$ in the absence of double exchange for the ij iron sites pair.

Table I. 300-MHz ^{1}H NMR Shifts and T_1 Values at 300 K for the Isotropically Shifted Signals of the Reduced HiPIP from *Chromatium vinosum*

signal	δ (ppm)	T_1[a] (ms)	assignment[b]
a	16.8	2.4	β-CH_2 (v)
b	15.9	6.6	β-CH_2 (z, x)
c	12.7	6.5	β-CH_2 (w, v)
d	11.6	2.3	β-CH_2 (e)
e	10.7	2.2	β-CH_2 (d)
f	10.1	9	?
v	8.3	22	? (c)
w	7.7	15	β-CH_2 (c)
x	7.4	9	? (b)
7	7.2	9	β-CH_2 (a)
z	5.3	6	β-CH_2 (b)

[a] Estimated by using the MoDEFT pulse sequence; the standard deviations for signals a-c are below 3%, for signals d-f are below 10%. Signals v-z are overlapping slow relaxing signal(s); however, the intensity plotted versus delay time displays a two exponential behavior which allows us to determine T_1 with a standard deviation <10%. [b] Letters in parentheses indicate the NOE connectivities with the partner of the β-CH_2 geminal pair underlined.

(48) Sandstrom, J. *Dynamic NMR Spectroscopy*; Academic: New York, 1982; Chapter 4.
(49) Gupta, R. K.; Redfield, A. G. *Biochem. Biophys. Res. Commun.* **1970**, *41*, 273.
(50) Zener, C. *Phys. Rev.* **1951**, *82*, 403.
(51) Anderson, P. W.; Hasegawa, H. *Phys. Rev.* **1955**, *100*, 675.
(52) Karpenko, B. V. *J. Magnetism Magnetic Materials* **1976**, *3*, 267-274.
(53) Girerd, J.-J. *J. Chem. Phys.* **1983**, *79*, 1776-1775.
(54) Belinskii, M. I.; Tsukerblat, B. S.; Gerbeleu, N. V. *Sov. Phys. Solid State* **1983**, *25*, 497-498.
(55) Noodleman, L.; Baerends, E. J. *J. Am. Chem. Soc.* **1984**, *106*, 2316-2327.
(56) Blondin, G.; Girerd, J. J. In press.
(57) Belinskii, M. I. *Mol. Phys.* **1987**, *60*, 793.
(58) Barbaro, P.; Bencini, A.; Bertini, I.; Briganti, F.; Midollini, S. *J. Am. Chem. Soc.* **1990**, *112*, 7238-7246.
(59) Papaefthymiou, G. C.; Laskowski, E. J.; Frota-Pessoa, S.; Frankel, R. B.; Holm, R. H. *Inorg. Chem.* **1982**, *21*, 1723-1728.
(60) Cerdonio, M.; Wang, R.-H.; Rawlings, J.; Gray, H. B. *J. Am. Chem. Soc.* **1974**, *96*, 6534.
(61) Sontum, S. F.; Noodleman, L.; Case, D. A. In *The Challenge of d and f Electrons, Theory and Computation*; Salahub, D. R., Zerner, M. C., Eds.; ACS Symposium Series; American Chemical Society: Washington, DC, 1989.

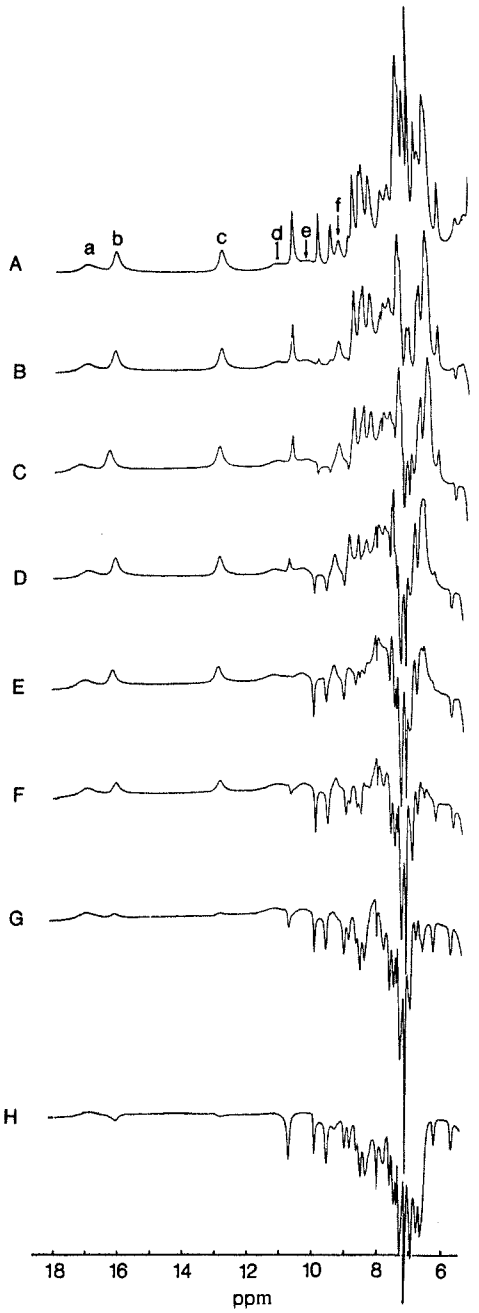

Figure 2. 300-MHz ^{1}H NMR spectra of reduced *Chromatium vinosum* HiPIP in D_2O pH 7.0 and 298 K: (A) reference spectrum at 300 MHz; traces from (B)–(H), spectra obtained by using the super-WEFT pulse sequence and different times τ of 60 (B), 40 (C), 25 (D), 15 (E), 10 (F), 5 (G), and 2.5 (H) ms, respectively.

Equation 9 is an extension of that already proposed by Noodleman.[36] The magnetic susceptibility can be calculated through the usual Van Vleck equation.[62]

^{1}H NMR Results

The 300-MHz ^{1}H NMR spectrum of reduced HiPIP from *Chromatium vinosum* is shown in Figure 2A, and the NMR parameters of the signals of interest are reported in Table I. Four isotropically shifted signals a–d are located in the 10–17 ppm region, as previously reported.[18] The super-WEFT sequence applied with different delay times allows us to identify further fast relaxing signals like e and f (Figure 2B–H). Most of these resonances can be reasonably assigned to the protons experiencing the closest contacts with the paramagnetic cluster, namely the β-CH_2 protons of the four cysteinyl ligands. In order to identify

(62) Griffith, J. S. *Structure and Bonding* **1972**, *10*, 87.

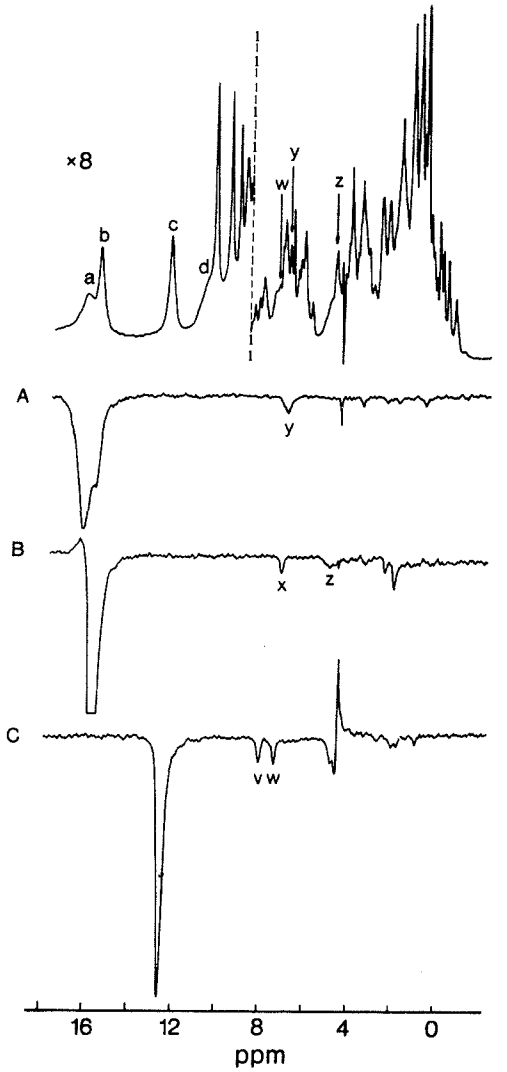

Figure 3. 300-MHz ^{1}H NMR spectra of reduced *Chromatium vinosum* HiPIP in D_2O pH 7.0 and 298 K: upper trace, reference spectrum; traces from (A)–(C) show steady-state NOE difference spectra obtained by saturating peaks a, b, and c, respectively. Signals y, z, and w correspond to signals h′, c′, and d′ of the oxidized protein, respectively (see Figures 4 and 5).

Table II. Steady-State Nuclear Overhauser Effects Measured[a] between the Isotropically Shifted Resonances of the Reduced HiPIP from *C. vinosum*

observed signals						saturated
e	v	w	x	y	z	signals
				4.1 (1.8)		a
			1.5 (2.2)		3.0 (1.8)	b
	4.6 (2.1)	5.5 (1.9)				c
<0.5						d

[a] The data were recorded at 300 MHz and 298 K and are reported as percent decrease in signal intensity. The connection d–e has been obtained from the saturation transfer experiments with the partially oxidized species. The calculated distances are reported in parentheses.

the four geminal β-CH_2 pairs, as previously reported for the oxidized form,[28] and try to rationalize the magnetic coupling and the spin distribution in the Fe_4S_4 cluster, we have carried out ^{1}H nuclear Overhauser effect experiments on the hyperfine shifted signals of reduced HiPIP and saturation transfer experiments on the same signals of the partially oxidized protein. The difference spectra obtained upon saturating resonances a, b, and c of reduced HiPIP are shown in Figure 3, and a map of the NOE connectivities is reported in Table II. Signals a, b, and c connect with resonances y, z, and w, respectively. Analysis of the relaxation profiles of the latter signals indicates that each one actually corresponds to

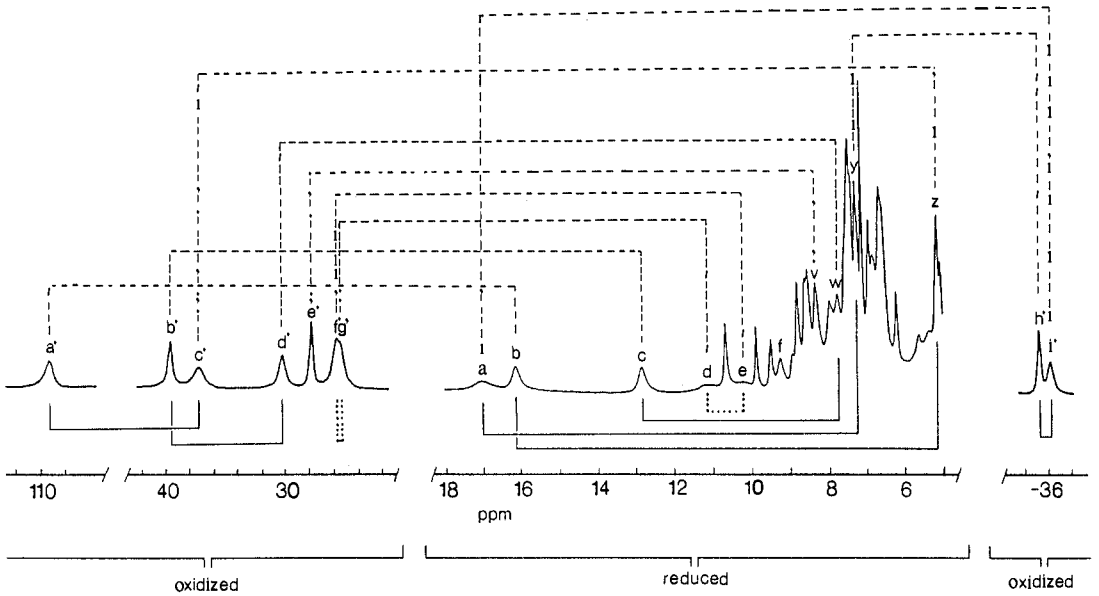

Figure 4. Schematic diagram of the saturation transfer connectivities (- -) between the hyperfine shifted resonances in the oxidized and the reduced HiPIP from *Chromatium vinosum*. The inferred (···) and experimental (—) NOE connectivities in the reduced and oxidized HiPIP are also indicated below the spectra. The a′–c′, b′–d′, and h′–i′ connectivities were already observed.[28]

at least two overlapped resonances, one of them having a T_1 of a few milliseconds. The interproton distances evaluated with eq 1, by using a τ_c value of 3.3×10^{-9} s obtained from the Stokes–Einstein relationship,[17] are in the range 1.7–1.9 Å, so the above pairs can be reasonably assigned to geminal β-CH_2 protons. The indetermination on the reorientational correlation time does not allow us to use this criterion to obtain proton–proton distances with an error smaller than 10%. However, this accuracy is enough to distinguish between β–β and α–β interactions. Furthermore, it is reasonable to expect NOE's between signals of geminal protons, which also are expected to have the shortest T_1's. The assignment of signals y, z, and w as β-CH_2 protons is confirmed by saturation transfer and EXSY experiments (see below). Signals b and c show further NOE connectivities with signals x and v, respectively (T_1 = 9–10 and 22 ms, respectively). The assignment of the latter signals is still dubious. The distances calculated from NOE experiments are 2.1–2.2 Å which are smaller than α-CH–β-CH distances; furthermore their shifts would be unusually large. Alternatively, protons of residues close to the cluster could experience a large shift and be close to the Cys β-CH_2 groups. Further experimental data are needed to assign such signals. Saturation of signals d, e, and f does not result in any appreciable and reproducible NOE.

Monodimensional saturation transfer and bidimensional EXSY NMR experiments allowed us to perform a full correlation among the hyperfine shifted signals of the reduced and oxidized systems. We have investigated the system at pH 5.2 where the protein is more stable in the oxidized state. The results of saturation transfer experiments on 50% oxidized HiPIP as well as the NOE connectivities in the oxidized and reduced species are schematically reported in Figure 4. In Figure 5 the 2D EXSY NMR spectrum of partially oxidized HiPIP ($\simeq$50%) is shown. Signals a, b, c, d, e, v, w, y, and z of reduced HiPIP correspond to signals i′, a′, b′, g′, f′, e′, d′, h′, and c′ of the oxidized form, respectively. These findings along with the NOE connectivities among the signals in the oxidized form previously described[28] are in complete agreement with the present NOE data. The signals b–z, c–w, e–d, and y–a in the reduced HiPIP and the signals a′–c′, b′–d′, f′–g′, and h′–i′ in the oxidized form, in the same order, are thus due to the Cys β-CH_2 geminal protons pairs. The absence of any NOE greater then 0.5% between signals d and e could be due to their short T_1 values (2.1–2.2 ms). The present data definitely assign the pairs of β-CH_2 geminal protons and show that one of such groups give rise to upfield shifted signals in the oxidized species. The correspondence of signal e′ of the oxidized form—the only signal experiencing a large isotropic shift not being assigned as a β-CH_2 geminal proton of a metal coordinated cysteine—with signal v of the reduced form, found in saturation transfer experiments, is further confirmed by the NOE c–v connectivity which matches with the b′–e′ connectivity already observed.[28]

The geminal protons should experience different shifts owing to the different dihedral angles ϕ between the Fe–S–C and the S–C–H planes,[63-65] as found from the X-ray structure.[66,67] In other Fe_4S_4 proteins like the oxidized ferredoxin from *Clostridium pasteurianum* (formally containing two Fe(II) and two Fe(III) ions) such dependence has been qualitatively accounted for.[27] In the present case we are observing a large shift separation between signals a and y in the reduced species, which becomes small in the oxidized species (signals h′ and i′). This is very relevant information which indicates that the difference between oxidized and reduced species may be due to a conformational change involving the β-CH_2 groups upon oxidation or to a different spin delocalization on the S–CH_2 moiety.[17,26,68] In the absence of a more complete assignment of the signals to particular residues, we do not further comment on this aspect, and we restrict ourselves to the discussion of the information obtained on the iron–sulfur clusters.

Discussion

The Oxidized HiPIP. This protein formally contains three Fe(III) and one Fe(II) ions. By referring to Figure 1 we label the iron(III) ions as 1, 2, and 3. The Mössbauer data show that one Fe(II)–Fe(III) pair is better described as $(Fe^{2.5+})_2$.[2-4] We label this pair the 3–4 pair. The local S for this pair is $S_{34} = {}^9/_2$. Again from Mössbauer data, it appears that the 1–2 pair has $S_{12} = 4$.[2,36] The hyperfine coupling between unpaired electrons and ^{57}Fe nuclei has been accounted for by Noodleman by using Hamiltonian (5) with the addition of a B_{34} term ($B_{34}/J = 2$) and $J > 0$, $\Delta J_{34} = 0$, and slightly positive ΔJ_{12} values.[36] We have anticipated that similar results for energies and wave functions can be obtained by taking $B_{34} = 0$, $J > 0$, and $\Delta J_{12} = -\Delta J_{34} > 0$[31] owing to the large correlation between J and B.[58,69] Figure

(63) Heller, C.; McConnell, H. M. *J. Chem. Phys.* **1960**, *32*, 1575.
(64) Ho, F. F.-L.; Reilley, C. N. *Anal. Chem.* **1969**, *41*, 1835.
(65) Stone, E. W.; Maki, A. H. *J. Chem. Phys.* **1962**, *37*, 1326.
(66) Carter, C. W.; Kraut, J.; Freer, S. T.; Alden, R. A. *J. Biol. Chem.* **1974**, *249*, 6339–6346.
(67) Freer, S. T.; Alden, R. A.; Carter, C. W.; Kraut, J. *J. Biol. Chem.* **1975**, *250*, 46–54.
(68) Unger, S. W.; Jue, T.; La Mar, G. N. *J. Magn. Reson.* **1985**, *61*, 448–456.
(69) Unpublished results from our laboratory.

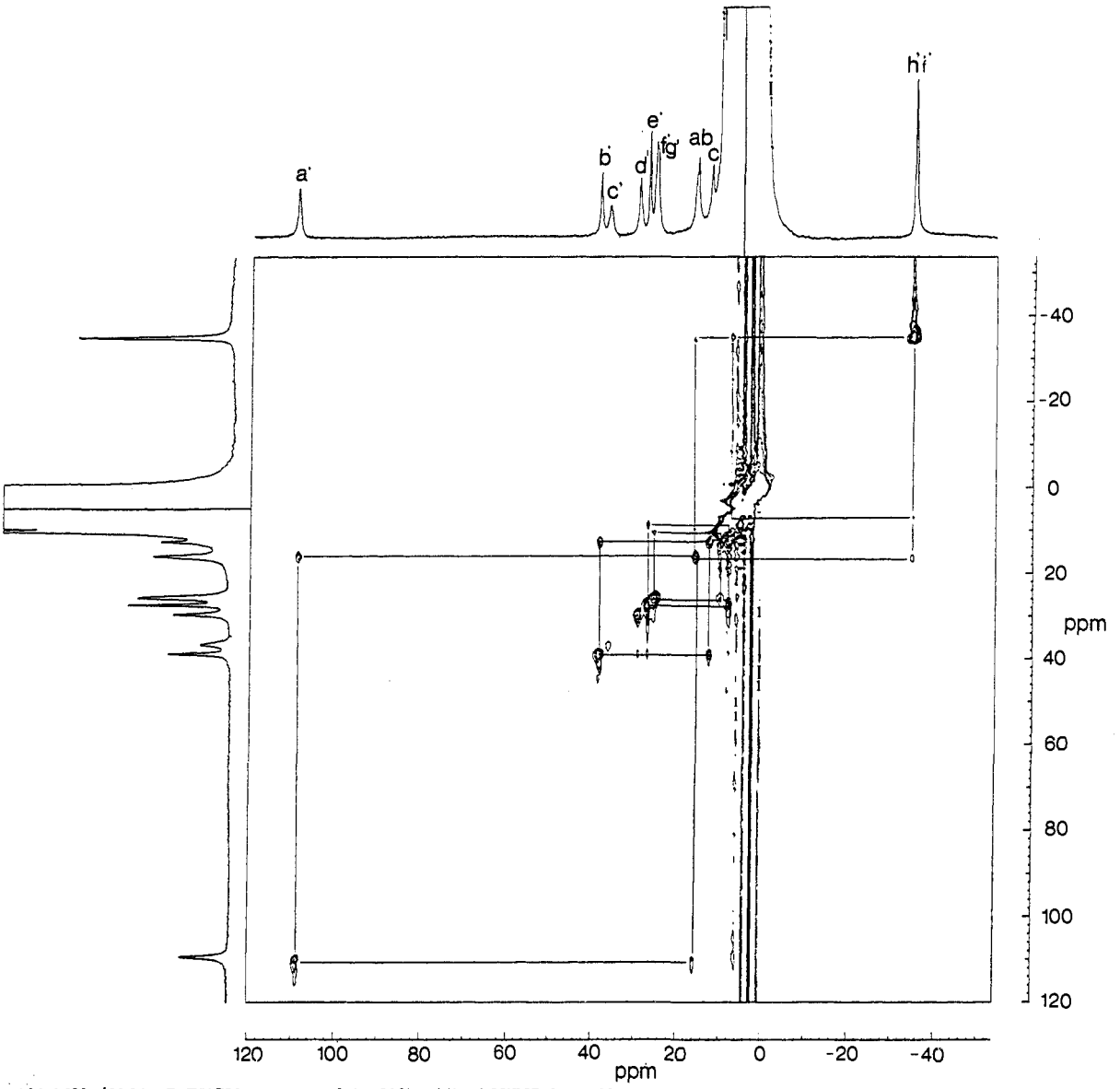

Figure 5. 300-MHz ^{1}H NMR EXSY spectrum of the 50% oxidized HiPIP from *Chromatium vinosum* at pH 5.2 in D_2O, in the −50/+120 ppm region, recorded with 7.5 ms mixing time. At this pH value the h′ and i′ peaks are accidentally degenerate. Peaks a and b are also ill-resolved under the present experimental conditions.

6A shows that the two choices of J and B values provide very similar temperature dependence of the individual $\langle S_{iz} \rangle$ values. Both treatments bring to an $S_{34} = {}^9/_2$ ground state as if the coupling within the mixed-valence pair were ferromagnetic in nature and $S_{12} = 4$. Figure 7 shows the energy levels for the two choices, i.e., as a function of increasing $\Delta J_{12}/J = -\Delta J_{34}/J$ for $B_{34}/J = 0$ or of increasing B_{34}/J for $\Delta J_{12}/J = \Delta J_{34}/J = 0$. In the former choice of parameters a delocalization term is not included. As already proposed,[34,35] any B_{34} value can account for delocalization, provided that $(S_{34} + {}^1/_2)B_{34} > \lambda^2/2k$.[56,70] Here λ is the vibronic constant and k is the force constant for the normal mode of vibration that correspond to the expansion and contraction of the coordination sphere when iron passes from the 3+ to the 2+ state and vice versa.[56]

Independently of the choice, two positive and two negative $\langle \mathbf{S}_{iz} \rangle$ values are easily obtained under a large range of J values, the positive one being that of the mixed-valence pair (Figure 6A). The $\langle \mathbf{S}_{3z} \rangle$ and $\langle \mathbf{S}_{4z} \rangle$ values under double exchange effects are equal, consistent with Mössbauer data. Differences should only be caused by low symmetry components. The temperature dependence of $\langle \mathbf{S}_{3z} \rangle$ and $\langle \mathbf{S}_{4z} \rangle$ is of Curie type, i.e., their values decrease with increasing temperature. In the symmetry of the used Hamiltonian, $\langle \mathbf{S}_{1z} \rangle$ and $\langle \mathbf{S}_{2z} \rangle$ are equal. It is expected that low symmetry components (not present in Hamiltonian (5)) make them different. For $J/kT > 1$ the temperature dependence of $\langle \mathbf{S}_{1z} \rangle$ and $\langle \mathbf{S}_{2z} \rangle$ is of anti-Curie type, i.e., they increase with increasing temperature. The temperature dependence of $\langle \mathbf{S}_{iz} \rangle$ provides information on to what extent the population of excited electronic states plays a role.

The ^{1}H NMR spectra of oxidized *Chromatium vinosum* HiPIP show six downfield signals and two upfield signals. Four of the downfield signals show decreasing shifts with increasing temperature and therefore are assigned to the mixed-valence pair Fe_3–Fe_4 (Figure 6B). Their differing shifts are likely to be essentially due to different hyperfine coupling constants (e.g., different Fe–S bonds or different ϕ values of eq 10 within a β-CH_2). The remaining four signals belong to the two β-CH_2's of Fe_1(III) and Fe_2(III). With decreasing temperature $\langle \mathbf{S}_{1z} \rangle$ and $\langle \mathbf{S}_{2z} \rangle$ are predicted to decrease and even become negative. If still positive, the shift is downfield, and the temperature dependence is of anti-Curie type, as found for signals f′ and g′; if negative, an upfield shift is expected, as found for signals h′ and i′ (Figure 6B). The temperature dependence in this latter case is misleadingly of opposite sign, with respect to the former case, but originates from anti-Curie behavior. We term this behavior

(70) Girerd, J. J.; Papaefthymiou, V.; Surerus, K. K.; Munck, E. *Pure Appl. Chem.* **1989**, *61*, 805–816.

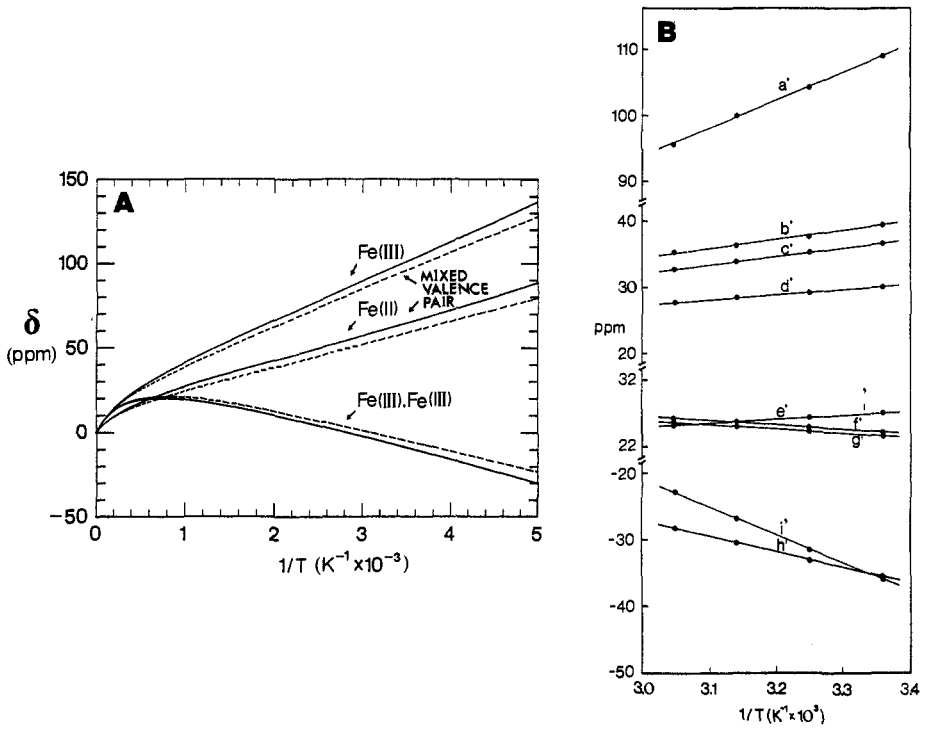

Figure 6. (A) Temperature dependence of the ^{1}H NMR isotropic shifts of oxidized HiPIP calculated by using eq 8 with $J = 300$ cm^{-1}, $\Delta J_{12} = 100$ cm^{-1}, $\Delta J_{34} = -100$ cm^{-1} and $B_{34} = 0$ cm^{-1} (—) or $J = 300$ cm^{-1}, $\Delta J_{12} = 100$ cm^{-1}, $\Delta J_{34} = 0$ cm^{-1}, and $B_{34} = 300$ cm^{-1} (--) ($Fe_1 = Fe_2 = Fe_3 = Fe(III)$ and $Fe_4 = Fe(II)$). (B) Experimental temperature dependence of the isotropically shifted signals of oxidized HiPIP from *Chromatium vinosum* at pH 7.0.[25]

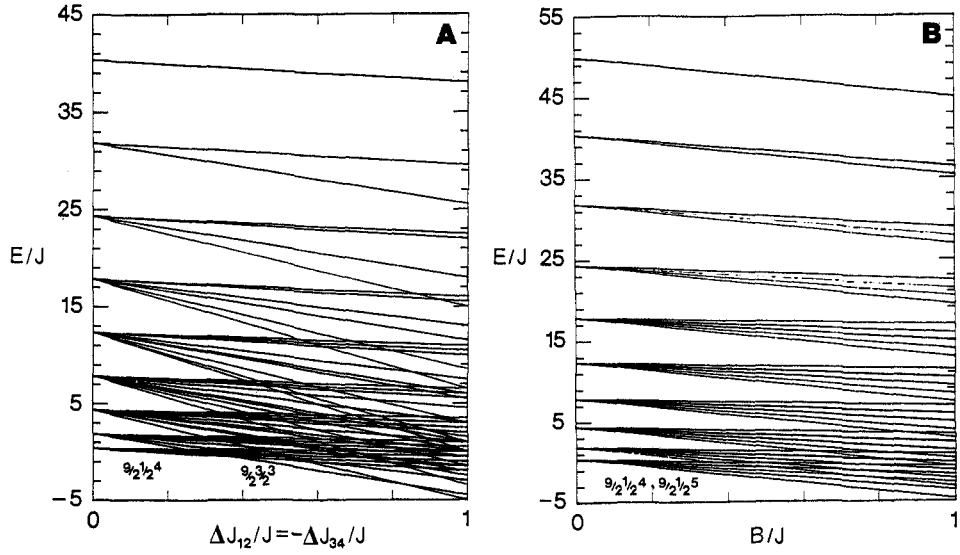

Figure 7. Energy levels for the 3Fe(III)–1Fe(II) system (oxidized HiPIP) calculated by using eq 7 with (A) $B_{34}/J = 0$ and $\Delta J_{12}/J = -\Delta J_{34}/J$ ranging from 0 to 1 or (B) $\Delta J_{12}/J = \Delta J_{34}/J = 0$ and B_{34}/J ranging from 0 to 1. Only the states that decrease in energy as a function of the variable parameters are shown. The ground states are indicated with their S_{34}, S, and S_{12}, values, respectively. The degeneracy of the ground level in (B) is removed by any $\Delta J_{12}/J > 0$ value.[36]

"pseudo-Curie". The experimental spectra of oxidized HiPIP II from *Ectothiorhodospira halophila* has indeed four upfield shifted signals with a "pseudo-Curie" temperature dependence.[23] The apparent puzzle of Cys β-CH_2 protons experiencing upfield shifts can be accounted for by the negative $\langle S_{iz} \rangle$ values imposed by the antiferromagnetic coupling of the iron(III) ions with the mixed-valence pair.

Note the analogy with reduced Fe_2S_2 proteins. In the case of reduced Fe_2S_2 proteins the "large" $S = {}^5/_2$ spin of Fe(III), because of antiferromagnetic coupling, induces a negative value of $\langle S_{iz} \rangle$ on the "small" $S = 2$ spin of Fe(II) at sufficiently high J/kT values.[29,31] In the present case the "large" $S_{34} = {}^9/_2$ spin of the mixed pair induces negative $\langle S_{iz} \rangle$ values for the other Fe(III) ions ($S_{12} = 4$), again at sufficiently high J/kT values. The present interpretation is based on the independent information from the Mössbauer hyperfine couplings which indicate an $S_{34} = {}^9/_2$ and $S_{12} = 4$ ground state.

The Reduced HiPIP. The 2Fe(II)–2Fe(III) clusters occur in reduced HiPIP's and oxidized Fd's. They are characterized by an $S = 0$ ground state due to antiferromagnetic coupling among the four irons.[2,5,11] The ^{1}H NMR spectra of the several systems are similar.[18,71,72] They are characterized by small shifts, relatively short T_1 and anti-Curie dependence of the hyperfine shifts (Figure

(71) Poe, M.; Phillips, W. D.; McDonald, C. C.; Lovenberg, W. *Proc. Natl. Acad. Sci. U.S.A.* **1970**, *65*, 797.
(72) Ho, C.; Fung, L. W.-M.; Wiechelman, K. J. *Methods Enzymol.* **1978**, *54*, 192.

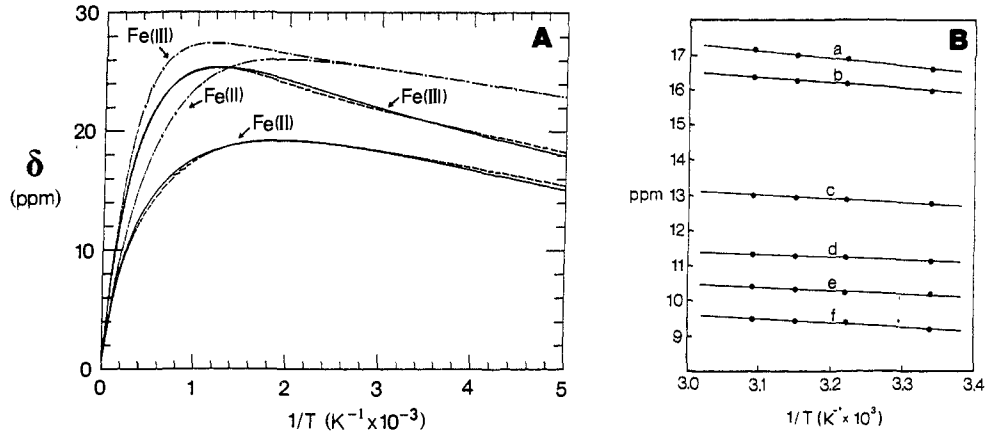

Figure 8. (A) Temperature dependence of the ^{1}H NMR isotropic shifts of reduced HiPIP calculated by using eq 8 with J = 400 cm^{-1}, $\Delta J_{12} = \Delta J_{34}$ = −200 cm^{-1}, and $B_{12} = B_{34}$ = 0 cm^{-1} (—), or J = 400 cm^{-1}, $\Delta J_{12} = \Delta J_{34}$ = 0 cm^{-1}, and $B_{12} = B_{34}$ = 400 cm^{-1} (– –) ($Fe_1 = Fe_3$ = Fe(III) and $Fe_2 = Fe_4$ = Fe(II)), or J = 200 cm^{-1}, $\Delta J_{12} = \Delta J_{34}$ = 200 cm^{-1}, and $B_{12} = B_{34}$ = 0 cm^{-1} (– – –) ($Fe_1 = Fe_2$ = Fe(III) and $Fe_3 = Fe_4$ = Fe(II)). For each choice of parameters the upper curve corresponds to Fe(III), whereas the lower curve corresponds to Fe(II). (B) Experimental temperature dependence of the isotropically shifted signals of reduced HiPIP from *Chromatium vinosum* at pH 7.0.[25]

8B). The average magnetic moment is about 4 μ_B per cluster.[8-13] Furthermore, Mössbauer data indicate that all ions essentially behave as $Fe^{2.5+}$ ions.[2-4] At variance with the oxidized HiPIP case, anti-Curie behavior of all signals and the correct order of magnitude of magnetic susceptibility can be easily reproduced even with all J's equal, provided relatively large J values (≥400 cm^{-1}) are used. This is not surprising, since any system exhibiting S = 0 ground state will eventually display full anti-Curie behavior, independently of the presence or absence of electron delocalization. If, by analogy with the oxidized case, the electron delocalization is described in terms of two $S = {}^9/_2$ mixed valence pairs. The experimental data can be accounted for with certain orders of J values: for example, by using J = 200 cm^{-1} and $\Delta J_{12} = \Delta J_{34}$ = 200 cm^{-1} (see Figure 1, Fe_1 and Fe_2 = Fe(III), Fe_3 and Fe_4 = Fe(II)). Similar results are obtained by labeling $Fe_1 = Fe_3$ = Fe(III), $Fe_2 = Fe_4$ = Fe(II), and using J values of 400 cm^{-1} and $\Delta J_{12} = \Delta J_{34}$ = −200 cm^{-1}. In the latter models, there is again covariancy between B and J values (Figure 8A).

Further Considerations

We have performed sample calculations to further clarify the above points. Figure 7 shows the full scheme of the energy levels for the oxidized protein. Calculations are performed with or without the use of B parameters. For example, the effects of B on the oxidized system with $\Delta J_{12} > 0$ and $\Delta J_{34} = 0$ are also obtained without the use of B by reducing the J values of the mixed-valence pair ($\Delta J_{34} < 0$). The present NMR data cannot discriminate between the two choices.

However, the following considerations make the use of large B values somewhat arbitrary in the absence of independent data on the magnitude of double exchange. The J values measured in reduced Fe_2S_2 systems (Fe(III)–Fe(II)) are always found smaller than those measured in the same systems when oxidized (Fe(III)–Fe(III)).[73] If we use the same values in, for example, oxidized HiPIP for one Fe(III)–Fe(III) and one Fe(III)–Fe(II) pairs, respectively, keeping the other four J values intermediate, we find that this choice induces an $S_{34} = {}^9/_2$ ground state in the latter pair (as if it experienced ferromagnetic coupling) and an S_{12} = 4 ground state in the oxidized pair; an $S = {}^9/_2$ ground state is the prerequisite for facile electron spin delocalization ($(S_{34} + {}^1/_2)B_{34} > \lambda^2/2k$).[56] This may explain why delocalized mixed-valence pairs are so common in Fe_3S_4 and Fe_4S_4 clusters, whereas localized Fe^{2+}–Fe^{3+} centers are always observed in Fe_2S_2 clusters. Indeed, electron delocalization in dimers requires either ferromagnetic coupling,[74] which is relatively less common, or very large B/J values.[75] Another relevant piece of information is contained in the temperature dependence of the isotropically shifted signals of oxidized HiPIP (Figure 6B). The marked difference in the sign of the temperature dependence shows that little averaging occurs by chemical exchange between isomers experiencing double exchange alternatively on one or another of the three possible mixed-valence pairs. Apparently, the intrinsic asymmetry induced by the protein favors double exchange (possibly through differences in the J values) on one of the three possible mixed valence pairs.

Finally, we note that the T_1 values of the ^{1}H NMR signals of the reduced protein are, on the average, a factor of two shorter than in the oxidized protein. This is surprising for two reasons. First, Fe(II) has much shorter electronic relaxation times (and hence smaller nuclear relaxing ability) than Fe(III),[17] and in the reduced proteins there are two Fe(II) centers instead of one. Second, the system has a sizably reduced paramagnetism already at room temperature and this should also decrease the nuclear relaxation rates. We feel that this is due to long electronic relaxation times as a consequence of the electronic structure of the cluster.

Concluding Remarks

The ^{1}H NMR spectra of reduced HiPIP from *Chromatium vinosum* have been recorded under various conditions in order to reveal the broad signals of cysteine β-CH_2. Steady-state ^{1}H NOE measurements have allowed us to recognize three pairs of geminal protons. Saturation transfer studies have related the signals of the oxidized with those of the reduced species. In this way *all* geminal pairs of protons have been assigned in both reduced and oxidized species. The temperature dependence of the shifts in the reduced species has an anti-Curie behavior as already shown.[18-25] This may be accounted for on the basis of strong antiferromagnetic coupling among the four ions or of strong antiferromagnetic coupling between more weakly antiferromagnetically coupled Fe(II)–Fe(III) pairs, that show $S = {}^9/_2$ ground states.

The oxidized protein shows the puzzling property of having proton signals of a β-CH_2 group upfield. Upfield shifted signals appear to be a common feature in the NMR spectra of oxidized HiPIP's.[22-25] The antiferromagnetic coupling between Fe(III) on the one hand and the $S = {}^9/_2$ ground state in the Fe(II)–Fe(III) pair on the other hand may account for upfield shifts in this type of systems. Also, it appears that the temperature dependence is fully consistent with the proposed theoretical model. ^{1}H NMR spectra, together with NOE experiments which relate proton signals within each geminal proton pair, is a powerful tool in the investigation of iron–sulfur clusters. Of course, the NMR spectra

(73) Palmer, G.; Dunham, W. R.; Fee, J.; Sands, R. H.; Iizuka, T.; Yonetani, T. *Biochem. Biophys. Acta* **1971**, *245*, 201.
(74) Sacconi, L.; Mealli, C.; Gatteschi, D. *Inorg. Chem.* **1974**, *13*, 185.
(75) Drueke, S.; Chaudhuri, P.; Pohl, K.; Wieghardt, K.; Ding, X.-Q.; Bill, E.; Sawaryn, A.; Trautwein, A. X.; Winkler, H.; Gurman, S. J. *J. Chem. Soc., Chem. Commun.* **1989**, 59–62. Ding, X.-Q.; Bominaar, E. L.; Bill, E.; Winkler, H.; Trautwein, A. X.; Drueke, S.; Chaudhuri, P.; Wieghardt, K. *J. Chem. Phys.* **1990**, *92*, 178.

contain a further wealth of information related to the dihedral angle between the Fe-S-C and S-C-H planes and between interproton distances in both oxidized and reduced species. This information is being investigated also through comparison of the spectra of HiPIPs from different organisms.

Acknowledgment. We thank J.-J. Girerd for a long and stimulating discussion about the subtle interplay between the J and B parameters. We also thank L. Noodleman for clarifying to us the formalism used in eqs 7 and 9. Early suggestions by A. Bencini about the possibility of using only J values as parameters are also acknowledged.

Registry No. L-Cys, 52-90-4.

N-Bonded Copper(II)-Imino Nitroxide Complexes Exhibiting Large Ferromagnetic Interactions

Dominique Luneau,[1a] Paul Rey,*[,1a] Jean Laugier,[1a] Pascal Fries,[1a] Andrea Caneschi,[1b] Dante Gatteschi,[1b] and Roberta Sessoli[1b]

Contribution from the Laboratoires de Chimie (UA CNRS 1194), Département de Recherche Fondamentale, Centre d'Études Nucléaires, 38041 Grenoble, France, and the Department of Chemistry, University of Florence, Italy. *Received June 19, 1990*

Abstract: The magnetic interactions between copper(II) and imino nitroxide free radicals have been investigated in two novel adducts of copper(II)-bis(hexafluoroacetylacetonato): bis(μ-1,3-(2-phenyl-4,4,5,5-tetramethyl-4,5-dihydro-1*H*-imidazolyl-1-oxy))hexakis(hexafluoroacetylacetonato)tricopper(II) (**1**) and (2-(2-pyridyl)-4,4,5,5-tetramethyl-4,5-dihydro-1*H*-imidazolyl-1-oxy)bis(hexafluoroacetylacetonato)copper(II) (**2**). The crystal and molecular structures of both compounds have been determined. In **1**, the three metal ions are linked by two μ-1,3 bridging nitroxide ligands, the two external copper ions are in trigonal-bipyramidal environments with the imino nitroxide nitrogen atom coordinated in the basal plane, while the central metal ion is axially coordinated by the two nitroxide oxygen atoms. In **2**, the imino nitroxide and the imino pyridyl nitrogen atoms are both equatorially bound to the octahedral copper ion; in addition, the molecules interact in pairs in the crystal lattice. In both cases, the high-temperature magnetic behavior is governed by a large ferromagnetic interaction, $J > 300$ cm^{-1} ($H = -JS_iS_j$), which develops within the imino coordinated metal ion and the free radical. By contrast, the low-temperature magnetic properties strongly depend on weak additional interactions corresponding to the binding of the nitroxide oxygen to the central metal ion in **1**, and to the intermolecular short contact between the uncoordinated NO groups in **2**. The ferromagnetic coupling of spins is rationalized as arising from the exchange interaction of unpaired electrons in orthogonal magnetic orbitals. This situation is the consequence of the binding geometry of the imino nitroxide nitrogen atom to the copper(II) ion. Crystal data. **1**: $a = 12.740$ (4) Å, $b = 16.269$ (5) Å, $c = 19.470$ (6) Å, $\alpha = 78.89$ (1)°, $\beta = 78.30$ (1)°, $\gamma = 81.00$ (1)°, triclinic, $P\bar{1}$. **2**: $a = 9.317$ (4) Å, $b = 12.922$ (5) Å, $c = 13.525$ (6) Å, $\alpha = 95.24$ (1)°, $\beta = 109.71$ (1)°, $\gamma = 110.92$ (1)°, triclinic, $P\bar{1}$. This study shows that large ferromagnetic interactions between metal ions and nitroxide free radicals are possible; it opens new perspectives for the design of molecular high-spin species.

Among the strategies that have been developed for designing molecular ferromagnets,[2-6] the metal-radical approach[6] has led to promising results. This strategy is based on the building of chains of alternating antiferromagnetically coupled metal and organic spins of different magnitude leading to ferrimagnetic one-dimensional compounds. The solid-state properties of these materials depend on the interchain coupling, which is generally not a controlled process. However, using nitronyl nitroxides[7] (Figure 1) and manganese(II) ions we were able to prepare such ferrimagnetic chains, which were coupled in the solid state, leading to low-temperature ferromagnets.[8,9] The low transition temperatures in these materials may be accounted for by the bulkiness of the ligands surrounding the metal ion and the absence of exchange pathways between the chains. This results from the fact that bulky electron-withdrawing hexafluoroacetylacetonato groups are needed to induce the nitroxide bonding to the metal.

In spite of this limitation, the metal-radical approach is one of the most versatile strategies for preparing high-spin species by different coupling schemes. Although large antiferromagnetic interactions and ferrimagnetic extended derivatives are the rule in metal-nitroxide magnetochemistry, chains of ferromagnetically coupled copper ions and nitroxides have also been prepared.[10,11] Indeed, when a free radical is axially bound by its oxygen atom to a tetragonal copper(II) ion, a weak ferromagnetic interaction develops. This is the only case where such a coupling is observed. The magnitude of the interaction has been qualitatively studied by empirical theoretical methods;[12] it depends on the binding of the nitroxide, mainly the bonding distance, which is always large in this geometry. Therefore, it is now generally accepted that strong metal-nitroxide ferromagnetic interactions cannot be obtained by using nitronyl nitroxides.

Previous investigations of the magnetic properties of metal organic free radical complexes such as semiquinonates[13,14] and

(1) (a) Centre d'études nucléaires de Grenoble. (b) University of Florence.
(2) Sugawara, T.; Bandow, S.; Kimura, K.; Iwamura, H.; Itoh, K. *J. Am. Chem. Soc.* **1986**, *108*, 368.
(3) Torrance, J. B.; Oostra, S.; Nazzal, S. *Synth. Met.* **1987**, 709.
(4) Pei, Y.; Verdaguer, M.; Kahn, O.; Sletten, J.; Renard, J.-P. *J. Am. Chem. Soc.* **1986**, *108*, 7428.
(5) Miller, J. S.; Epstein, A. J.; Reiff, W. M. *Chem. Rev.* **1988**, *88*, 201.
(6) Caneschi, A.; Gatteschi, D.; Rey, P.; Sessoli, R. *Acc. Chem. Res.* **1989**, *22*, 392.
(7) Ullman, E. F.; Osiecki, J. H.; Boocock, D. G. B.; Darcy, R. *J. Am. Chem. Soc.* **1972**, *94*, 7049.
(8) Caneschi, A.; Gatteschi, D.; Rey, P.; Sessoli, R. *Inorg. Chem.* **1988**, *27*, 1756.
(9) Caneschi, A.; Gatteschi, D.; Renard, J.-P.; Rey, P.; Sessoli, R. *Inorg. Chem.* **1989**, *28*, 3914.
(10) Caneschi, A.; Gatteschi, D.; Laugier, J.; Rey, P. *J. Am. Chem. Soc.* **1987**, *109*, 2191.
(11) Cabello, C. I.; Caneschi, A.; Carlin, R. L.; Gatteschi, D.; Rey, P.; Sessoli, R. *Inorg. Chem.* **1990**, *29*, 2582.
(12) Caneschi, A.; Gatteschi, D.; Grand, A.; Laugier, J.; Pardi, L.; Rey, P. *Inorg. Chem.* **1988**, *27*, 1031.

0002-7863/91/1513-1245$02.50/0